ISSN 2347-3487

Correlation between microstructure, mechanical and thermal properties of In-Bi-Sn-Ag melt spun alloys

Rizk Mostafa Shalaby[1,*], Mohammed Younus[1, 2], Abu-Bakr El-Bediwi[1], and Mustafa Kamal[1]
[1] Metal Physics Lab., Physics Department Faculty of Science, Mansoura University, Mansoura, Egypt
*Corresponding author: doctorrizk2@yahoo.co.uk
kamal42200274@yahoo.com
baker_elbediwi@yahoo.com
Tel.: +2-01062507736
[2] On leave, M.Sc. student, Iraq
my_radi@live.com

Abstract

A series of indium-bismuth-tin-silver alloys containing up to 5 wt. % silver were quenched from melt by chill-block melt-spin technique. The resultant ribbons were studied by X-ray diffraction (XRD), scanning electron microscope (SEM), energy dispersive X-ray (EDX), and deferential scanning calorimetry (DSC) techniques. Structural, mechanical and thermal correlations were discussed and reviewed for In-Bi-Sn-Ag Field's metal alloy systems. The results are interpreted in terms of the phase changes occurring in the alloy system. It is found that melting point, solidus and liquidus temperatures of the solder alloys are lowered as the Ag content is increased. With the addition of Ag, the In rich phase is finer in size, and the intermetallic compounds are more uniformly distributed. As a result, Young's modulus and microhardness of In-Bi-Sn are increased when Ag is added into the solder alloy. It is also, concluded that from our results, the present work relates to a melting temperature adjustable metal thermal interface material (TIM) applicable to an interface between a microelectronic packaging component and a heat dissipation device, so as to facilitate the heat dissipation of the microelectronic component.

Keywords: Silver addition, Field's metal, x-ray diffraction, microstructure analysis, mechanical properties, thermal analysis.

Council for Innovative Research
Peer Review Research Publishing System
Journal: JOURNAL OF ADVANCES IN PHYSICS
Vol.8, No.1
www.cirjap.com, japeditor@gmail.com

ISSN 2347-3487

1. Introduction

The indium-bismuth-tin Field's metal system has attracted attention in recent years as it has potential application as a step soldering (Pb- free solder alloy) in the microelectronic industry. It is also a good model system for the study of rapid prototyping, die casting and soft solder formulation. The intent of this article is to continue and to explore the effects of silver additions on the structural, thermal and mechanical properties of In-Bi-Sn melt-quenched ribbons [1]. Nowadays, there is rapid development of technology in many industrial fields. Along with that, study and research is done to ensure that technology growth will not only make our daily routine easier but its application is safe. As far as our concern, we do not want human and environment become the victim of the unsafe technology. Simply said, we want the kind of technology which is secure for both human and environment. The development of low melting solder which is similar or lower melting point compared to eutectic Sn-Pb is becoming more famous among researchers especially for those who are involved in microelectronic industries. This is encouraged by higher demand for low temperature lead free solder to prevent the damage of electronic devices due to high operating temperature. At the same time by using low temperature lead free solder, it can terminate the use of lead for the safety of workers. Health and environmental problem due to the usage of toxic lead has attracted researchers to find alternative materials as a replacement of lead and other toxic element alloys. The focus is not just the termination of lead but also producing low temperature lead free alloys. Alloys which are considered as low melting are alloys with melting temperature between 50 ^{o}C to 180 ^{o}C [2]. Field's metal is one of the most important alloys with minimum toxicity. Surface mount technology (SMT) is demanding the use of low temperature solder alloy to prevent damages due to heat influence. Electronic devices used for SMT is sensitive to high temperature. Moreover, excessive heat can lead to damage of electronic components such as liquid crystal display (LCD) and circuit board. Ruggiero and Rutter [3] studied the microstructure of the ternary eutectic of the Bi–In–Sn system after solidifying thin specimens unidirectionally at very slow speeds of 0.74–53 mm/day. They were found that the structures consisted of two coarse two-phase eutectics of BiIn–γ Sn and Bi–γ Sn. Applying thermal, metallographic and x-ray analysis they found the temperature and liquid composition of a eutectic reaction involving Sn, Bi, and InBi. Stelmakh et al. [4] studied seven polythermal sections inside In-InBi-Sn region using differential thermal analysis and X-ray diffraction. Kabassis et al. [5] found eutectic temperature at 59 ^{O}C involving phases In_2Bi γ and β. They solidified the alloys directionally and characterized them by metallographic methods. Continuing their studies Kabassis et al. [6] in 1986 investigate the section of In_2Bi and a projection of the liquid surface is given. Specimens of eutectic Bi-InBi-γ at 77 ^{O}C were unidirectionally solidified at very low speed and quenched to form a representative solid/liquid interface in the study of Ruggiero et al. [7]. The interfacial microstructure and mechanical properties of a low melting temperature lead-free solder of $In_{18.75}Bi_{22.15}Sn$ (in at. %) were investigated by Huang et al. [8] the microstructure analysis of bulk In–Bi–Sn revealed that irregular lamellar c-Sn phases distributed in the In_2Bi matrix. There was only a single endothermic peak with an onset temperature of 62C^{o} on the DSC curve, indicating that In–Bi–Sn is close to a ternary eutectic alloy. The ultimate tensile strength was 21.76 MP and the elongation reached 87 %, indicating an excellent ductility of this alloys. S. W. Yoon et al. [9] investigated the phase equilibria in the Sn-Bi-In ternary alloy system, performed both by theoretical and experimental methods. Following the regular solution model and a standard thermochemical calculation, a theoretical evaluation of the phase equilibrium in the entire ternary system is conducted. The resulting phase diagram agrees well both with the existing data and with the data from the current experiments. However, different from previous findings, this study finds a non-binary nature of the Sn-BiIn and Sn-BiIn quasi-binaries and nine invariant reactions, one eutectic, six pertectic and two peritectoid. V.T. Witusiewicz et al. [10] were reported thermodynamic re-optimization of the Bi-In-Sn system based on new experimental data. A new thermodynamic description is presented in this study for the ternary Bi–In–Sn system in the entire composition range. Several vertical and isothermal sections as well as the liquidus surface and selected thermodynamic properties are calculated using the thermodynamic description. They show reasonably good agreement with previous reported experimental data Adam Lipchitz et al. [11] determined the specific heat of the eutectic alloys of the indium-bismuth-tin tertiary system using a differential scanning calorimeter technique and analyze the results to determine if the thermodynamic properties of the system have sufficient scaling for experimental modeling applications. The results verify the melting temperatures of the alloys (in 60 ^{o}C) and establish a relationship between temperature and specific heat. Mustafa Kamal et al. [12] have succeeded in producing sample of Sn-Bi-In by a rapid solidification processing, in which tin-bismuth-indium melt-spun alloy containing two phases distributed uniformly with the Sn-matrix. On the basis of their observations they prefer the Sn10Bi10In solder for intermediate-step soldering in hermetic packaging. Fann et al. in 2008 [13] invented a new Field's metal In-Bi-Sn alloy to provide a thermal interference material (TIM) applicable to an interference between microelectronic packaging component and heat dissipation device. Their invention relates to a melting temperature adjustable metal thermal interference material (TIM). The main purpose of our work is to investigate the effect of small additions of Ag on the melting temperature, microstructure, thermal and elastic properties on In-Bi-Sn eutectic Field's metal.

2. Experimental techniques

The experimental techniques utilized have been described in details [14-17] and will be repeated here only briefly. The materials used in the present work are In, Bi, Sn and Ag granules, and the starting purity was 99.99%. In_{51-x}-$Bi_{32.5}$-$Sn_{16.5}$-Ag_x (where X were varying from 0.5 to 5 wt. %) quenched from melt ribbons have been produced by a single aluminum roller coated with copper (200 mm in diameter) melt-spinning technique [18]. The process parameters such as, the ejection temperature and the linear speed of the wheel were fixed at 550 k and 30.4 ms^{-1} respectively. The material flow rate Q_f has been empirically found to be an important chill block melt-spin process variable and its dependence on readily adjustable apparatus parameters has been described by Liebermann [19]. In the present study this parameter is calculated from:

ISSN 2347-3487

$$Q_f = V_r W t \quad \ldots\ldots\ldots\ldots\ldots (1)$$

Where (V_r) is the ribbon or substrate velocity, (W) is the ribbon width and (t) the average thickness calculated by dividing the ribbon mass (*m*) by length (*l*), density (ρ) and width.

$$t = \frac{m}{lw\rho} \quad \ldots\ldots\ldots\ldots\ldots (2)$$

X-ray diffraction analysis was done on a Shimadzu x-ray diffractometer (DX-30), using Cu k_α radiation (λ=1.5406 Å) with Ni-filter. The microstructure analysis was carried out on a scanning electron microscope (SEM) of type (JEOL JSM-6510LV, Japan) operate at 30 KV with high resolution 3 nm. Differential scanning calorimetry (DSC) was carried out on a (SDT Q600, USA) with a heat rate $10^oC\ min^{-1}$.The temperature dependence of resistivity was carried out by the double-bridge methods [20]. The variation of temperature during the resistance temperature investigation was determined using a step-down transformer connected to a constructed temperature control. The heating was kept constant during all the investigations at 5 $K.min^{-1}$ [14]. The elastic moduli, internal friction and the thermal diffusivity of melt-spun ribbons were examined in air atmosphere with a modified dynamic resonance method [21]. The hardness of the melt-spun ribbons was measured using a digital Vickers microhardness tester (model FM-7, Japan), applying a load of 10 gf for 5 sec via a Vickers diamond pyramid [22].

3. Results and discussions

3.1 Structural analysis

Rapid quenching of metallic alloys from melt was first carried out by Pol Duwez et al [23,24]. They found that the rapid quenching extends the solid solubility limits and produce non-equilibrium phase or amorphous alloys [25]. Fig.1 (a-j) shows the x-ray diffraction pattern of spun In_{51-x}-$Bi_{32.5}$-$Sn_{16.5}$-Ag_x (where X were varying from 0.5 to 5 wt. %) ribbons rapidly quenched from melt (500 ^oC). This technique is used to determine the degree of crystallinity, unit cell shapes, and lattice parameters. The pattern shows the existence of different kinds of phases, tetragonal structure phases of In-phase, Sn-phase, InBi-phase, In_3Sn-phase, $InSn_{19}$ phase and BiSn phase also Bi-phase with rhombohedral (hex) structure, Ag-phase with cubic structure and Ag_3Sn-phase with orthorhombic structure.

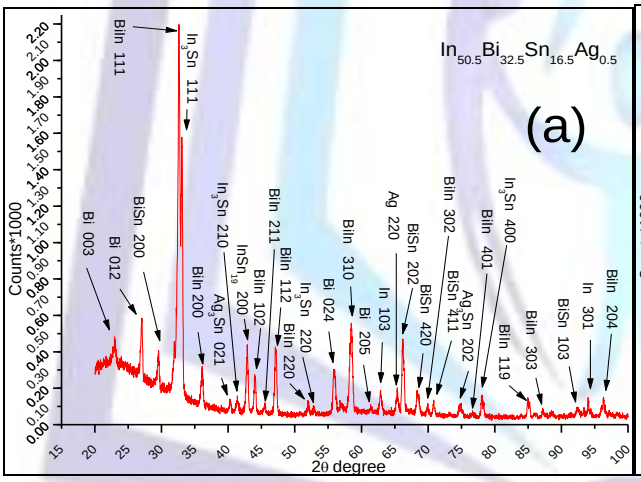

Fig. (1-a): X-Ray diffraction pattern of In-32.5Bi-16.5Sn-0.5Ag

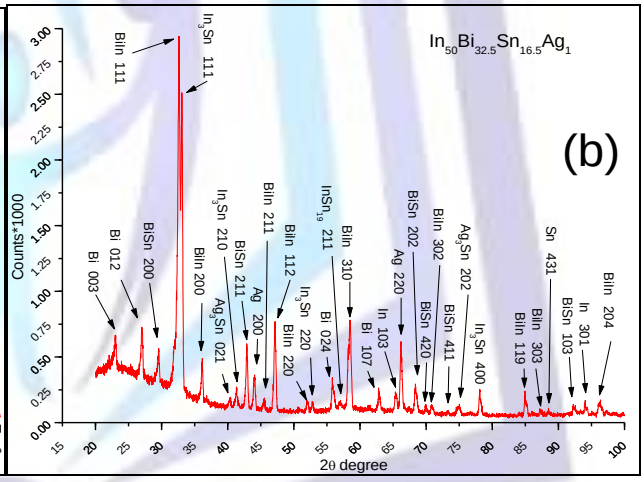

Fig. (1-b): X-Ray diffraction pattern of In-32.5Bi 16.5Sn-1Ag

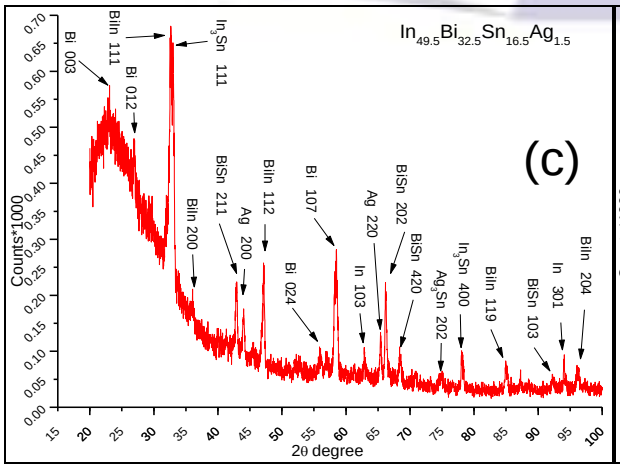

Fig. (1-c): X-Ray diffraction pattern of In-32.5Bi-16.5Sn-1.5Ag

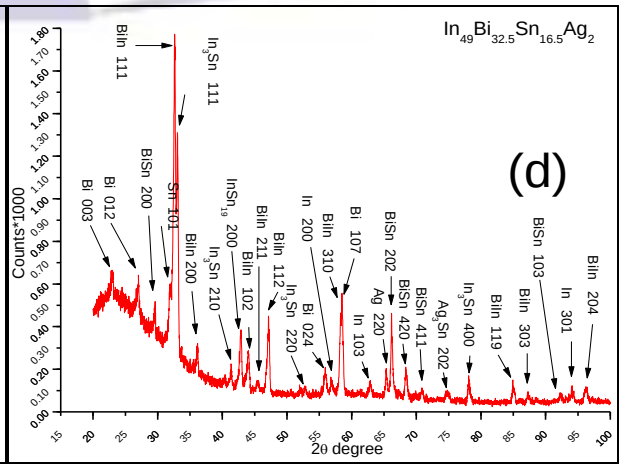

Fig. (1-d): X-Ray diffraction pattern of In-32.5Bi-16.5Sn-2Ag

ISSN 2347-3487

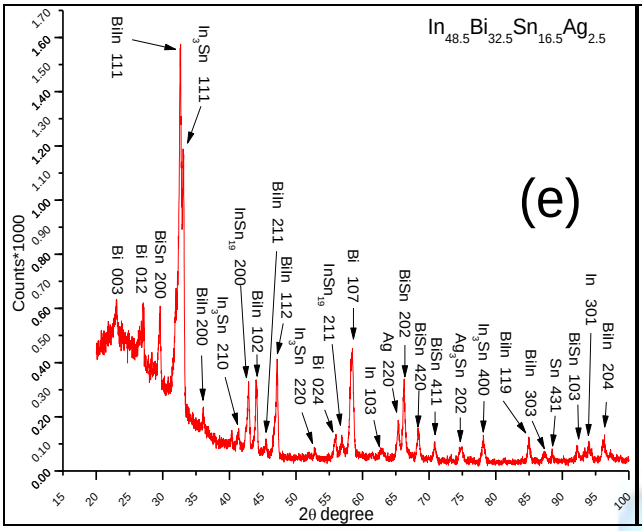

Fig. (1-e): X-Ray diffraction pattern of In-32.5Bi-16.5Sn-2.5Ag

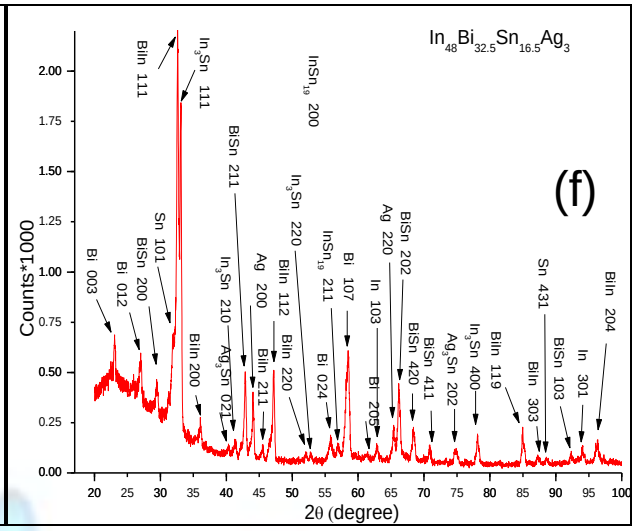

Fig. (1-f): X-Ray diffraction pattern of In-32.5Bi-16.5Sn-3Ag

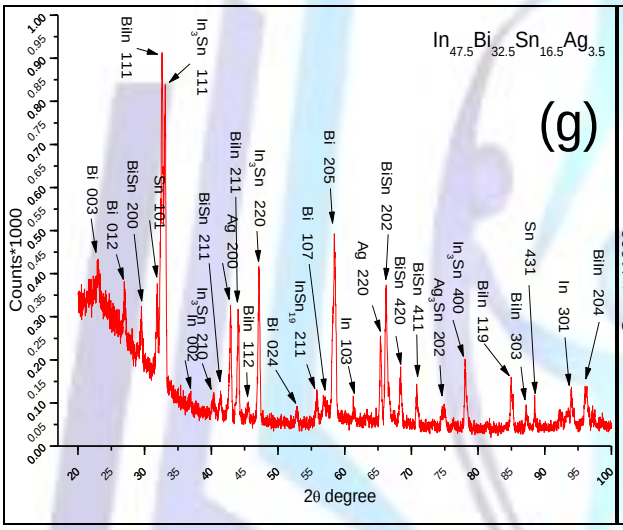

Fig. (1-g): X-Ray diffraction pattern of In-32.5Bi-16.5Sn-3.5Ag

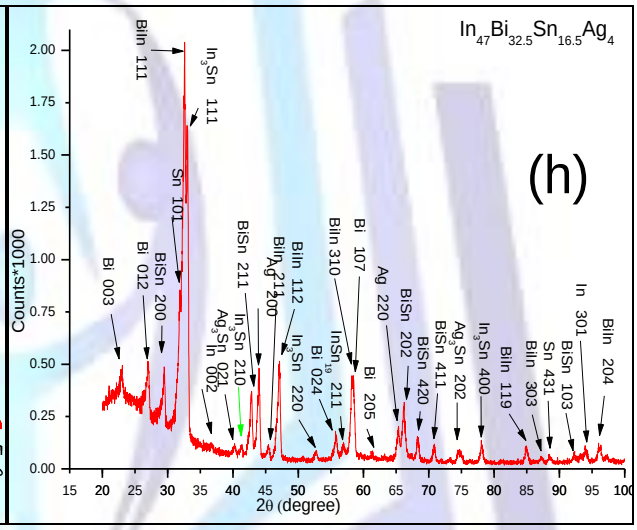

Fig. (1-h): X-Ray diffraction pattern of In-32.5Bi-16.5Sn-4Ag

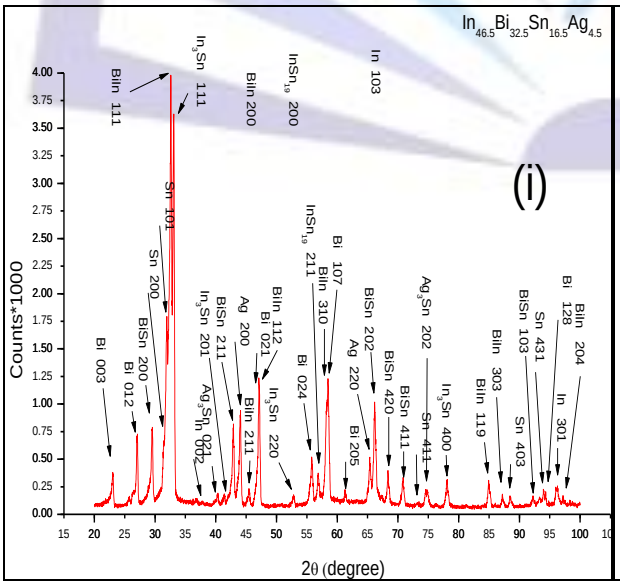

Fig. (1-i): X-Ray diffraction pattern of In-32.5Bi-16.5Sn-4.5Ag

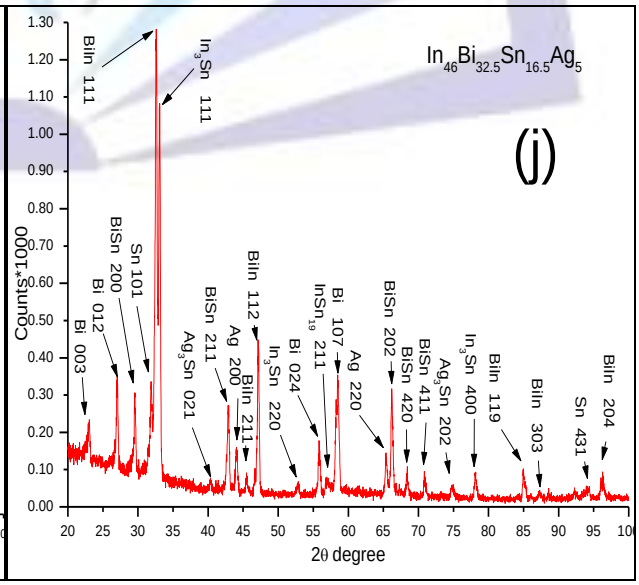

Fig. (1-j): X-Ray diffraction pattern of In-32.5Bi-16.5Sn-5Ag

ISSN 2347-3487

Table 1: Lattice parameters, number of atoms per unit cells and particle size of indium of all melt spun alloys

System	a (Å)	c (Å)	c / a	Cell volume($Å^3$)	Density (g/cm^3)	No.of atoms per unit cells	Particle size(Å)
$In_{50.5}Bi_{32.5}Sn_{16.5}Ag_{0.5}$	3.2961	4.9585	1.5044	53.8700	6.129	1.36	254.4614
$In_{50}Bi_{32.5}Sn_{16.5}Ag_{1}$	3.3081	4.9219	1.4878	53.8633	5.992	1.33	254.7852
$In_{49.5}Bi_{32.5}Sn_{16.5}Ag_{1.5}$	3.2564	4.9851	1.5308	52.8638	5.834	2.16	188.6618
$In_{49}Bi_{32.5}Sn_{16.5}Ag_{2}$	3.3074	4.9240	1.4888	53.8625	5.949	1.32	272.1447
$In_{48.5}Bi_{32.5}Sn_{16.5}Ag_{2.5}$	3.2935	4.9472	1.5021	53.6638	6.031	1.34	202.5792
$In_{48}Bi_{32.5}Sn_{16.5}Ag_{3}$	3.3685	4.9451	1.4681	56.1097	5.965	1.32	302.4848
$In_{47.5}Bi_{32.5}Sn_{16.5}Ag_{3.5}$	3.2841	4.9306	1.5013	53.1792	4.567	1.00	306.5600
$In_{47}Bi_{32.5}Sn_{16.5}Ag_{4}$	3.2800	4.9961	1.5232	53.7496	6.124	1.36	279.7264
$In_{46.5}Bi_{32.5}Sn_{16.5}Ag_{4.5}$	3.2872	4.9228	1.4975	53.1957	5.818	1.27	272.5864
$In_{46}Bi_{32.5}Sn_{16.5}Ag_{5}$	3.2906	4.9237	1.4963	53.3133	6.778	1.49	298.9752

The variation of the axial ratio (c/a) for indium phase with the variation of Ag concentration is listed in Table 1. The particle size is determined from x-ray diffraction pattern by using Scherer's equation $D_{hkl}= 0.9\ \lambda/\beta_{hkl}\ \cos\theta$, where D_{hkl} is the particle size, λ is the wavelength of Cu Kα= 1.54056 A, θ is the reflection angle and β_{hkl} is the full width at half maximum (FWHM) [26]. The details of the XRD analysis are listed in Table 1.

3.2 Microstructure analysis

The scanning electron microscope images and energy dispersive X-ray analysis (EDX) of In_{51-x}-32.5Bi-16.5Sn-XAg (where X were varying from 0.5 to 5 wt. %) ribbons, are shown in Fig.2 (a-j).

ISSN 2347-3487

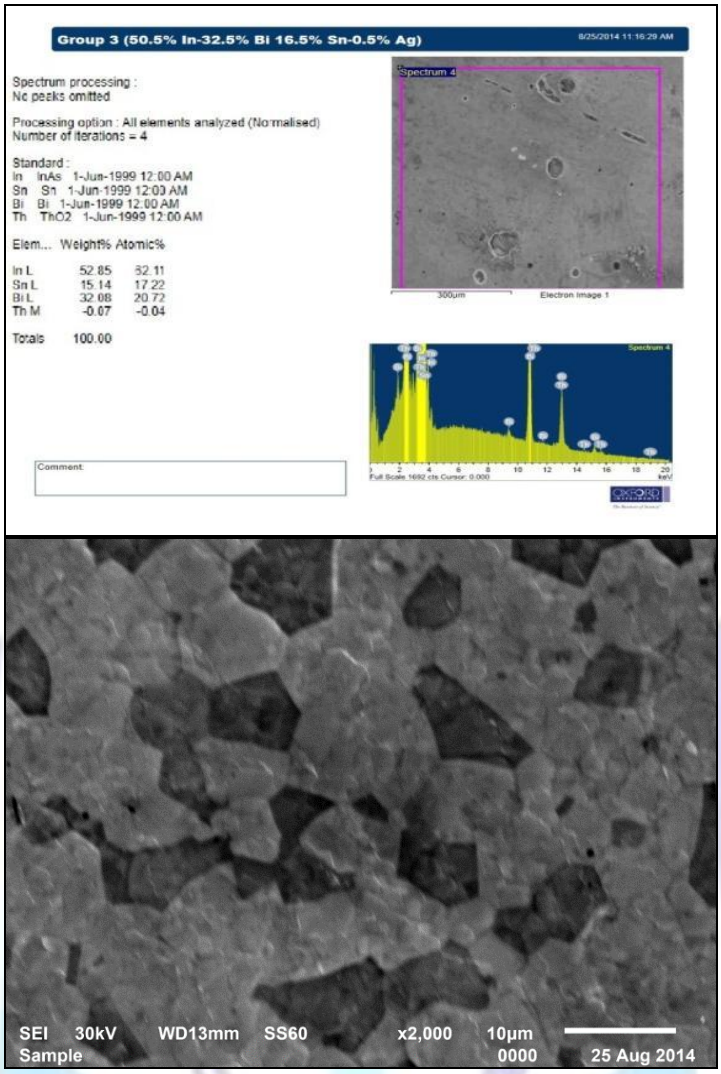

Fig. (2-a): EDX and SEM image of In-32.5Bi-16.5Sn-0.5Ag alloy

ISSN 2347-3487

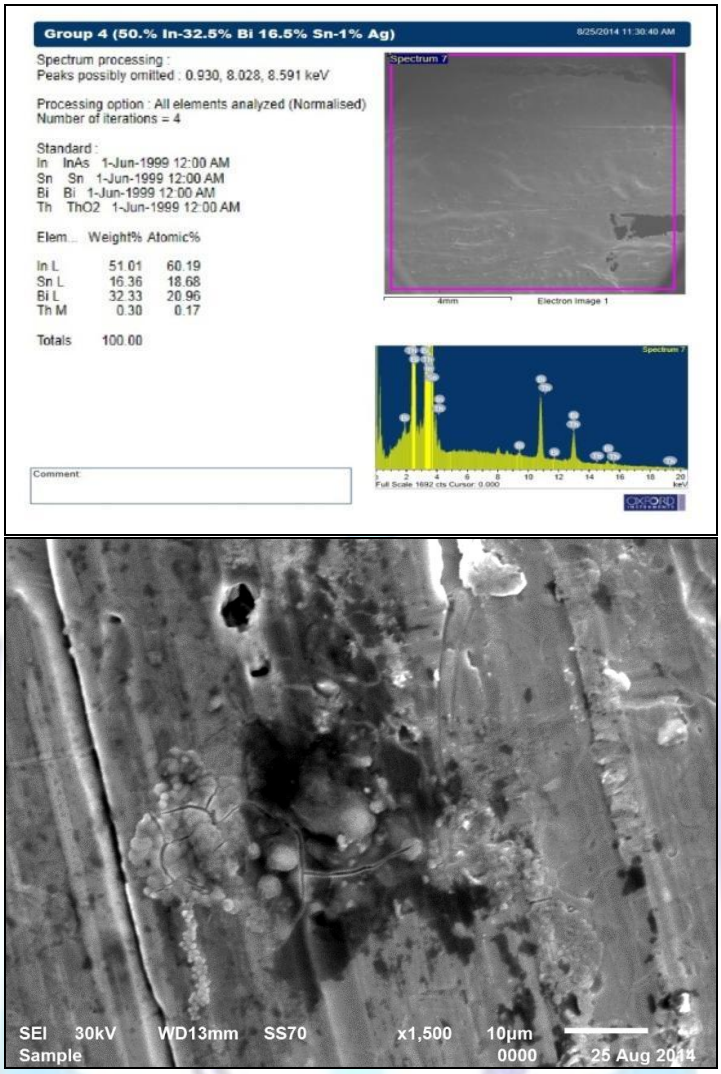

Fig. (2-b): EDX and SEM image of In-32.5Bi-16.5Sn-1Ag alloy

ISSN 2347-3487

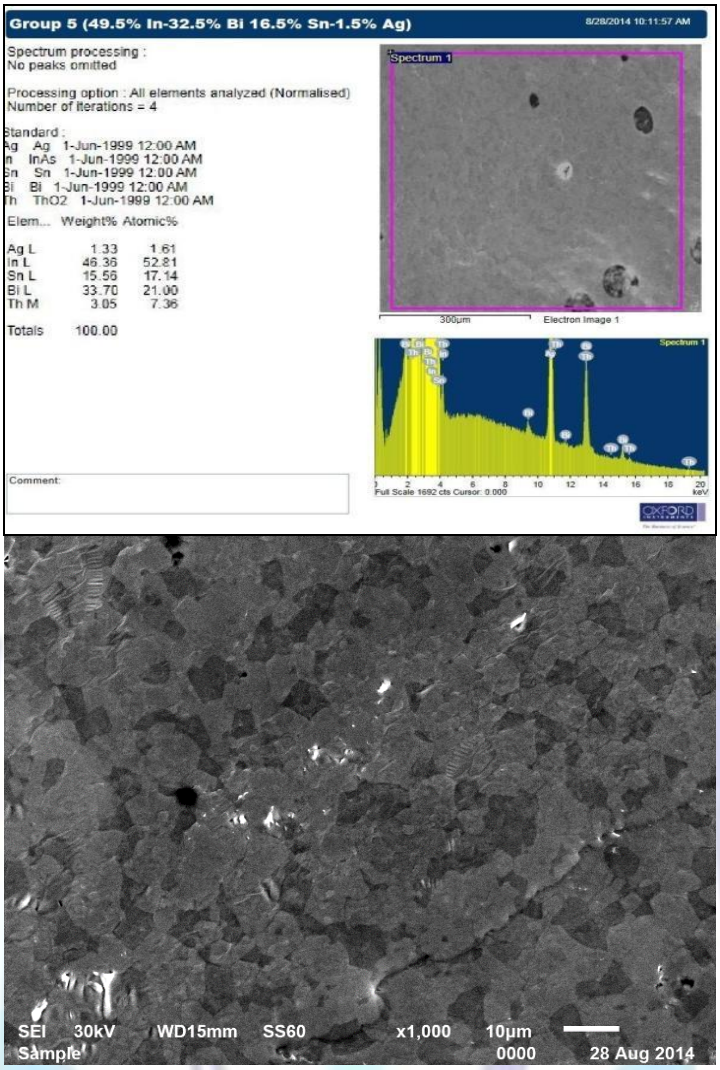

Fig. (2-c): EDX and SEM image of In-32.5Bi-16.5Sn-1.5Ag alloy

ISSN 2347-3487

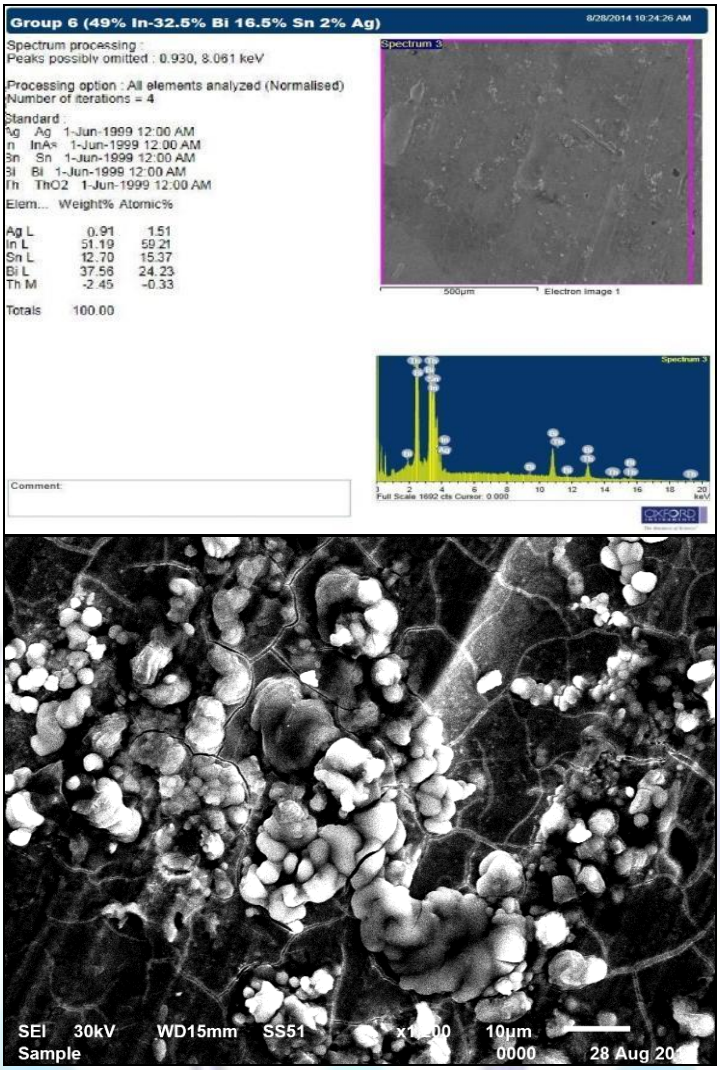

Fig. (2-d): EDX and SEM image of In-32.5Bi-16.5Sn-2Ag alloy

ISSN 2347-3487

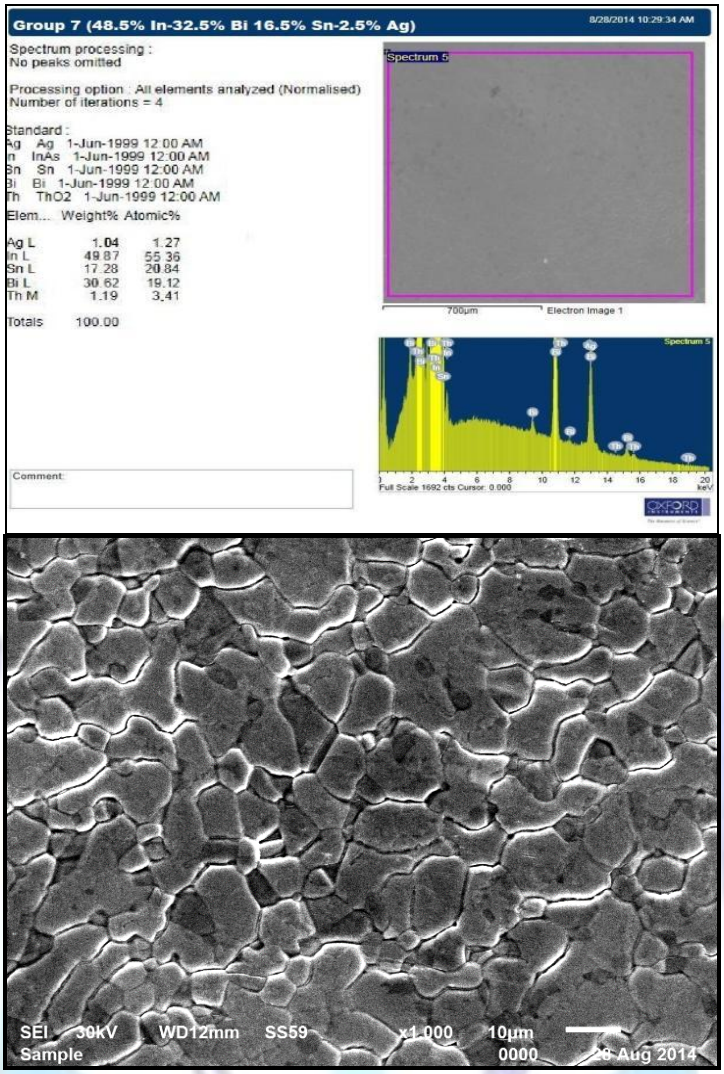

Fig. (2-e): EDX and SEM image of In-32.5Bi-16.5Sn-2.5Ag alloy

ISSN 2347-3487

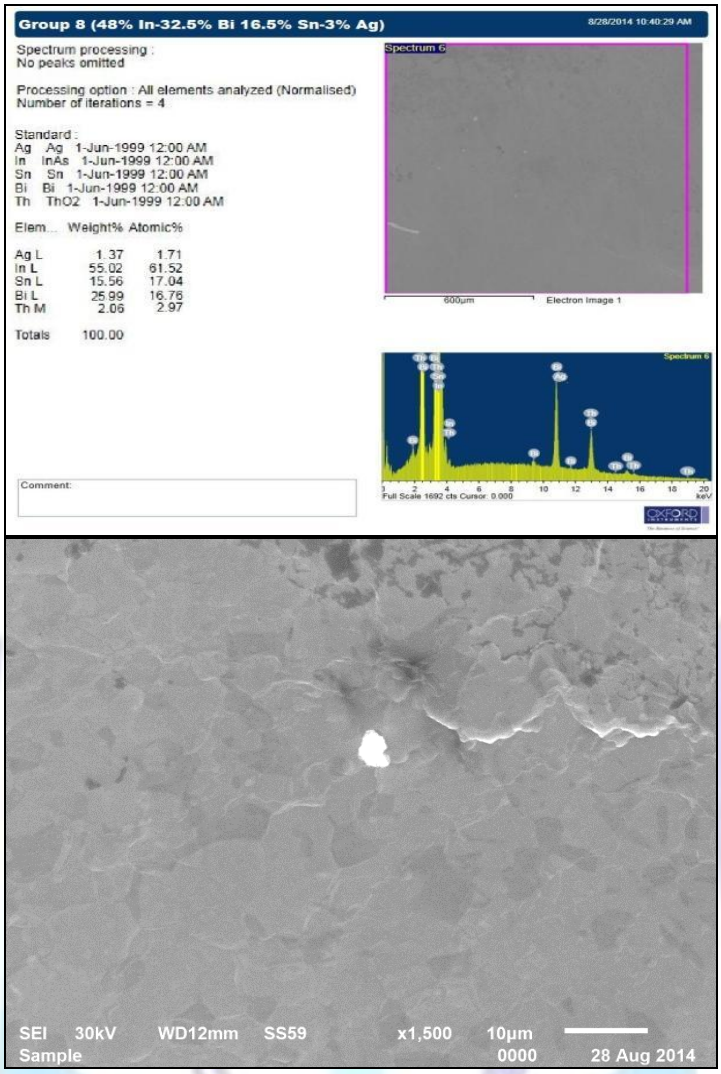

Fig. (2-f): EDX and SEM image of In-32.5Bi-16.5Sn-3Ag alloy

ISSN 2347-3487

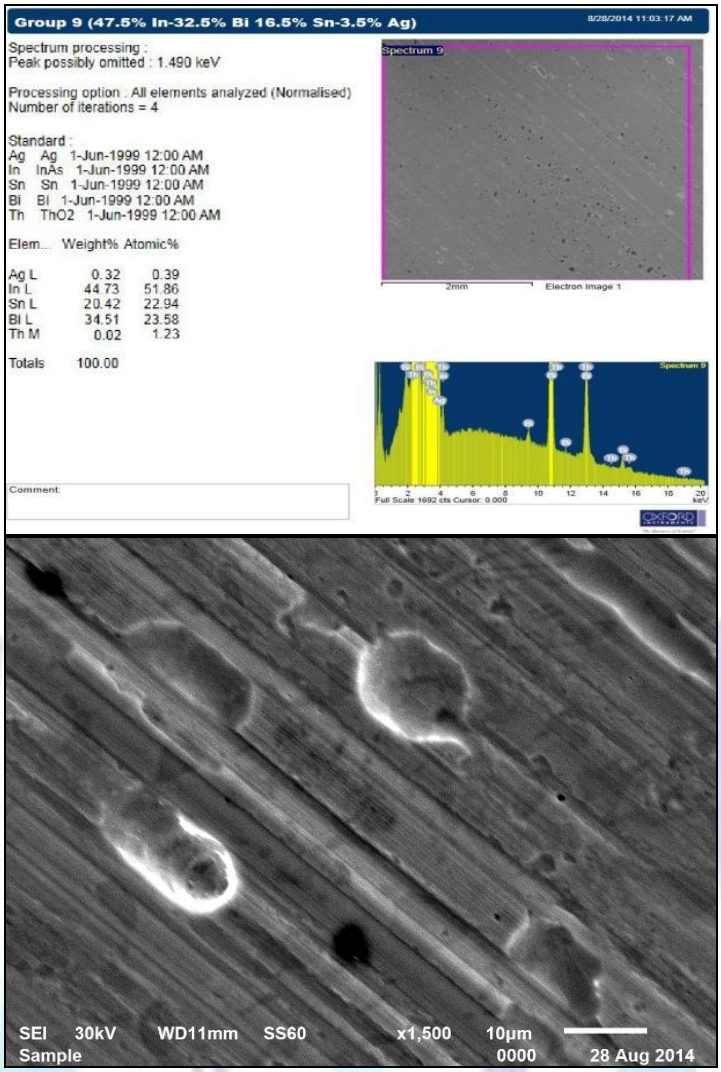

Fig. (2-g): EDX and SEM image of In-32.5Bi-16.5Sn-3.5Ag alloy

ISSN 2347-3487

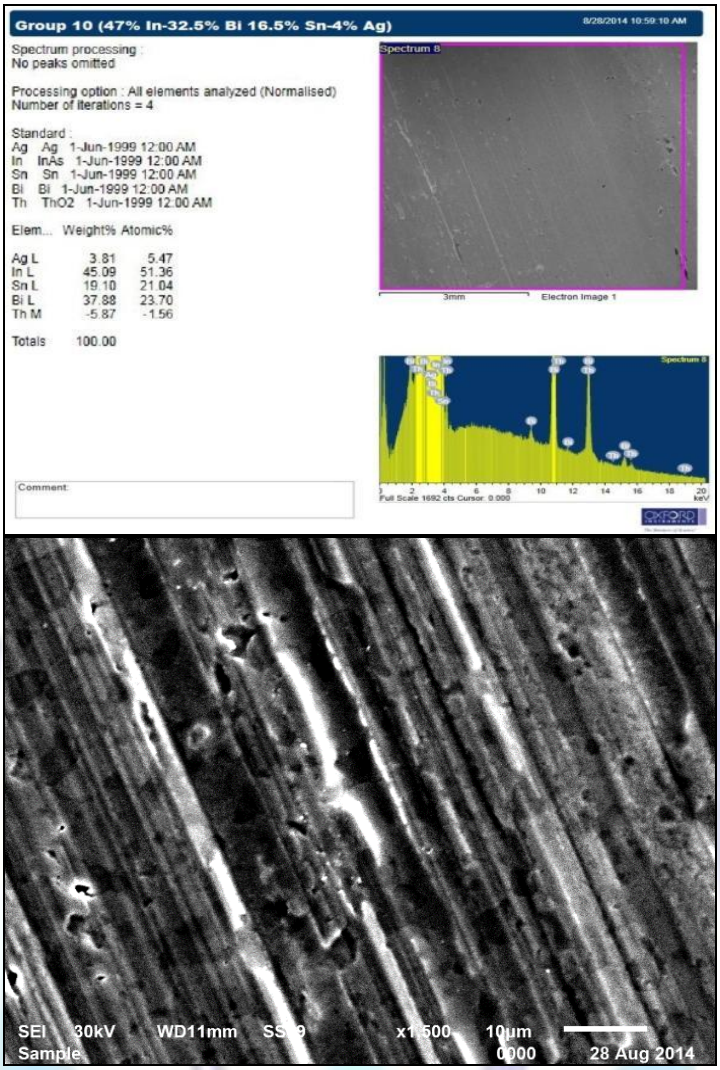

Fig. (2-h): EDX and SEM image of In-32.5Bi-16.5Sn-4Ag alloy

ISSN 2347-3487

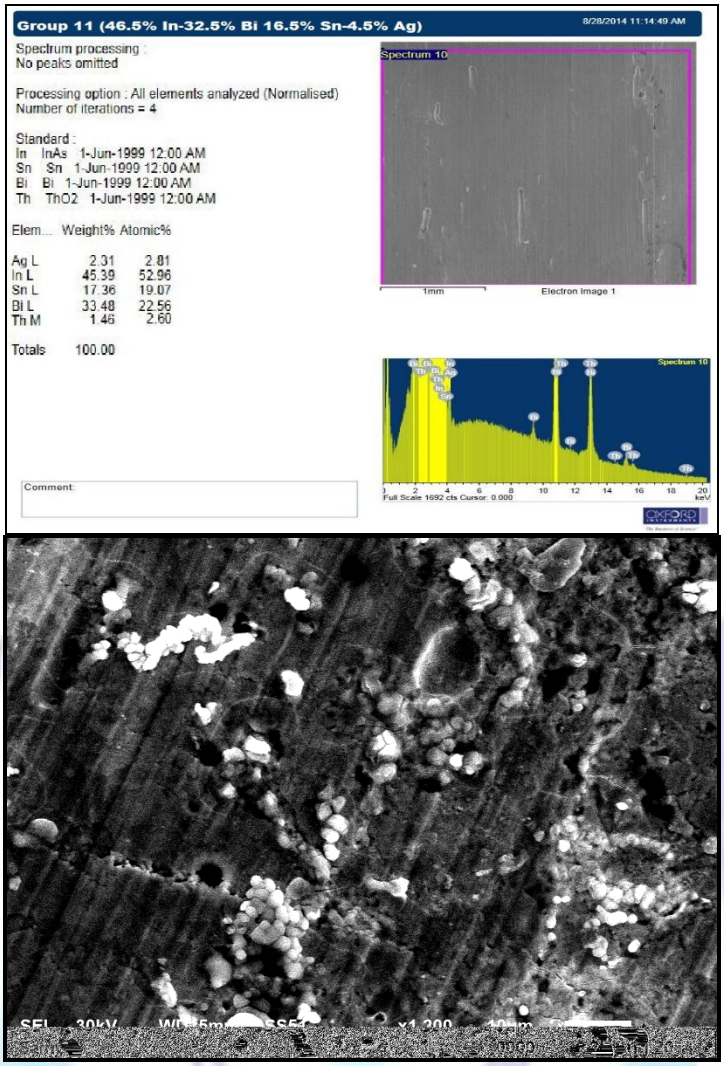

Fig. (2-i): EDX and SEM image of In-32.5Bi-16.5Sn-4.5Ag alloy

ISSN 2347-3487

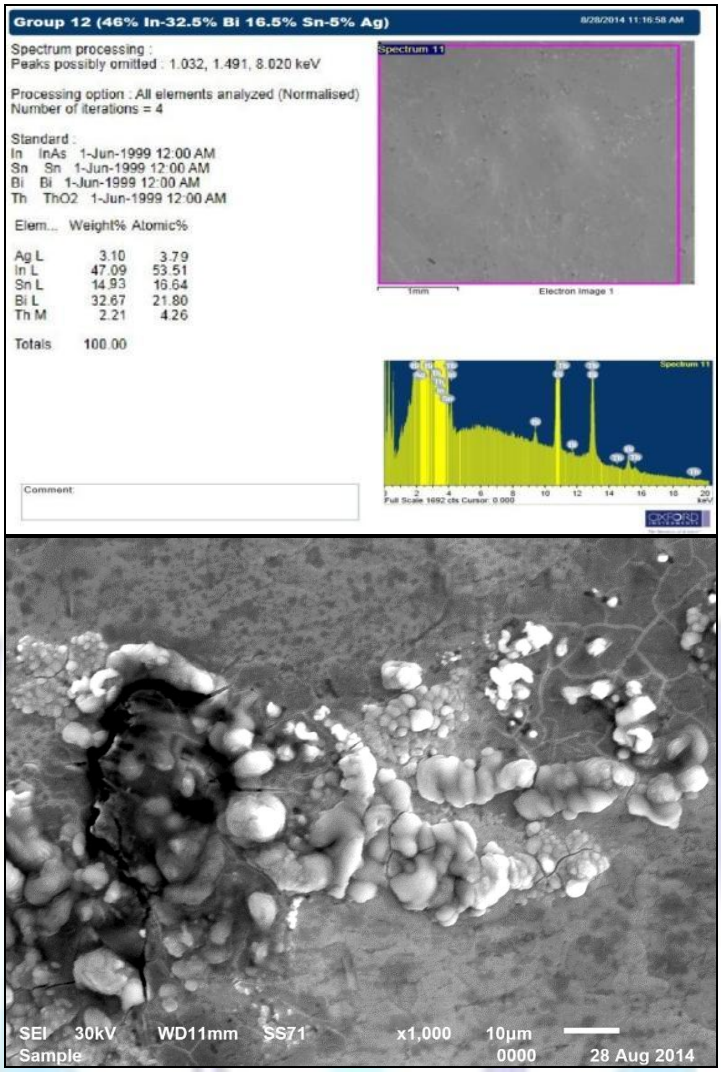

Fig. (2-j): EDX and SEM image of In-32.5Bi-16.5Sn-5Ag alloy

Fig.2 (a-j) shows microstructure of In-Bi-Sn-Ag, illustrate elemental (Bi, Sn and Ag) and intermetallic compounds distribution in matrix. The higher Ag content, leads to the finer In-rich phase, and the more uniform distribution of intermetallic compounds. So, the uniform microstructure improves the mechanical properties up to 3 wt. % Ag as indicated in table 3. The uniform microstructure of In-Bi-Sn-Ag is obtained when Ag is added into field's metal. This is due to the adsorption phenomenon during solidification process of an alloy [27].

3.3. Thermal analysis:

The melting temperature is a critical characteristic because it determines the maximum operating temperature of the system and the minimum processing temperature of the system and the minimum processing temperature which its components must survive. Melting temperature is a vital thermal property and has a strong influence on surface mount technology (SMT) field. A promising solder alloy should have a low melting temperature zone [28]. Huang [29] found that the onset point in the DSC heating curve represents the solidus temperature and that the peak point shows the liquidus temperature. Fig 3 (a-j) shows the DSC curves for In_{51-x}-32.5Bi-16.5Sn-XAg where X were varying from 0.5 to 5 wt. % alloy. Zu et al. [30] suggested that structural changes take place to some extent in molten alloys as a function of temperature, which have been confirmed by the corresponding calorific peak in a differential scanning calorimeter. So in this section, it is noted that further work is needed to probe the concrete change of structures with the help of a differential scanning calorimeter. Specimens approximately 7 mg in mass were cut from the melt-spun ribbons and were submitted to heating from room temperature to about 350c^{o} at rates of 10 $K.min^{-1}$ in a SDTQ600 differential scanning calorimeter DSC. A typical output is depicted in Fig. 3 (a-j) the results of the melting temperature, enthalpy, entropy change and the average specific heat are tabulated in Table (2**).** As we see from table (2) melting point for all quenched ribbons is around (50-60) c^{o} and there is a noticeable decrease in entropy change as we add silver with minimum value at 3.5 wt. % of silver addition also there is magnificent decrease in specific heat of In-Bi-Sn eutectic alloy when silver is add even in such small amount.

ISSN 2347-3487

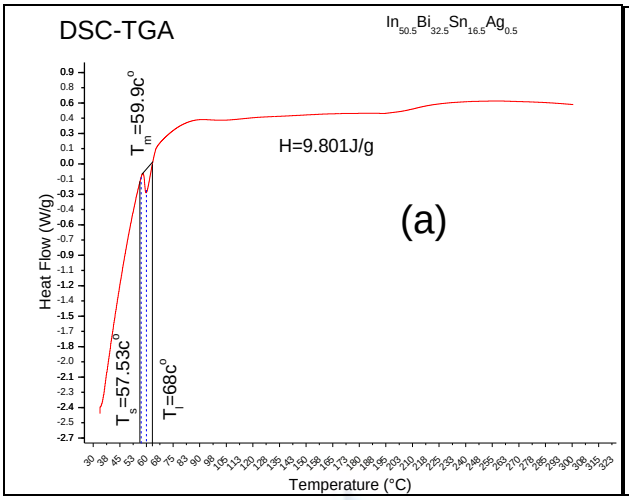

Fig. (3-a): DSC curve of In-32.5Bi-16.5Sn-0.5Ag

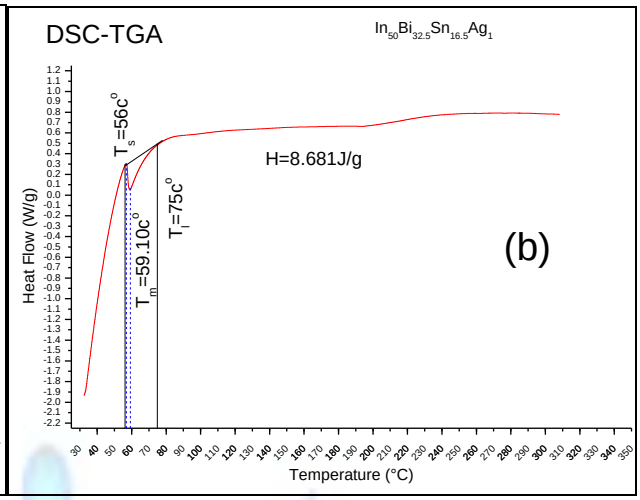

Fig. (3-b): DSC curve of In-32.5Bi-16.5Sn-5Ag

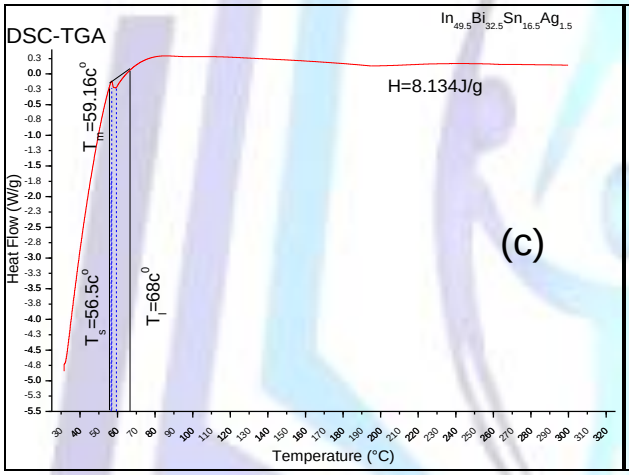

Fig. (3-c): DSC curve of In-32.5Bi-16.5Sn-1.5Ag

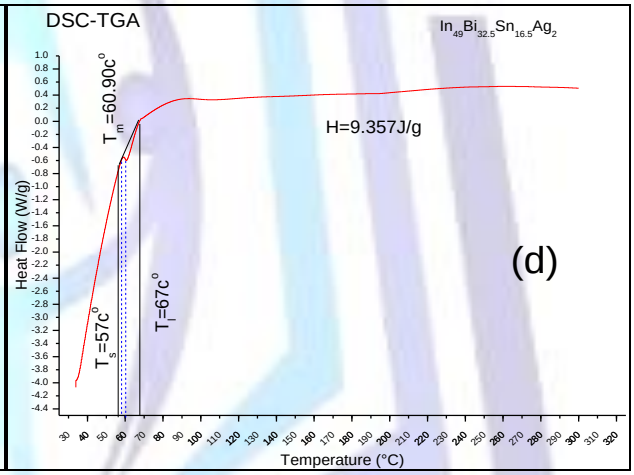

Fig. (3-d): DSC curve of In-32.5Bi-16.5Sn-2Ag

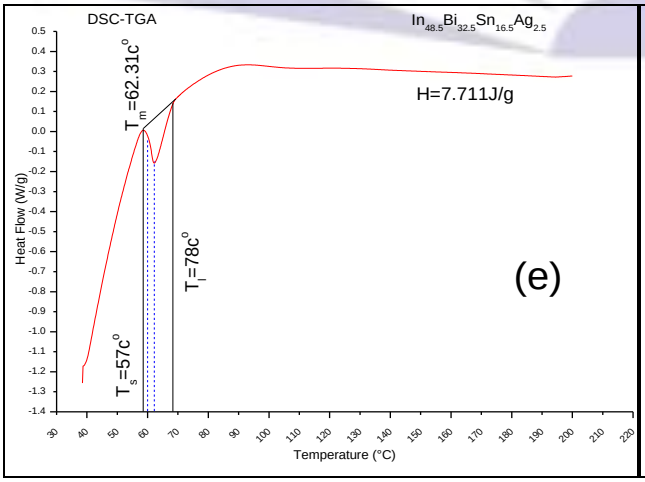

Fig. (3-e): DSC curve of In-32.5Bi-16.5Sn-2.5Ag

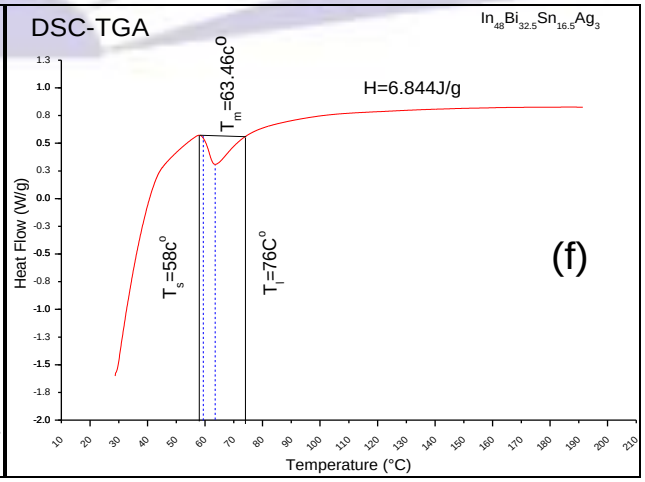

Fig. (3-f): DSC curve of In-32.5Bi-16.5Sn-3Ag

ISSN 2347-3487

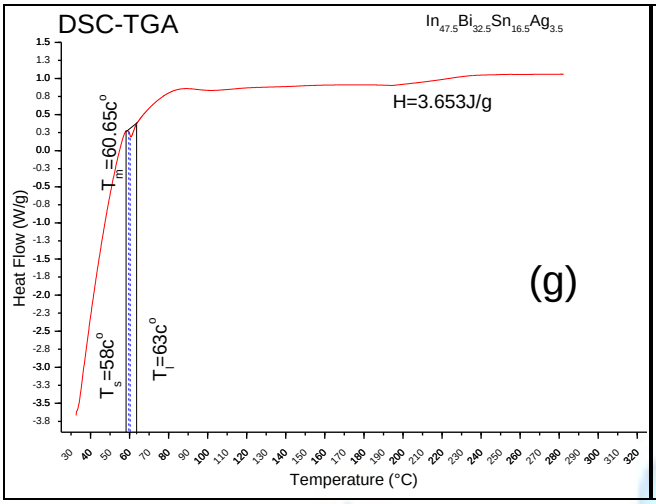

Fig. (3-g): DSC curve of In-32.5Bi-16.5Sn-3.5Ag

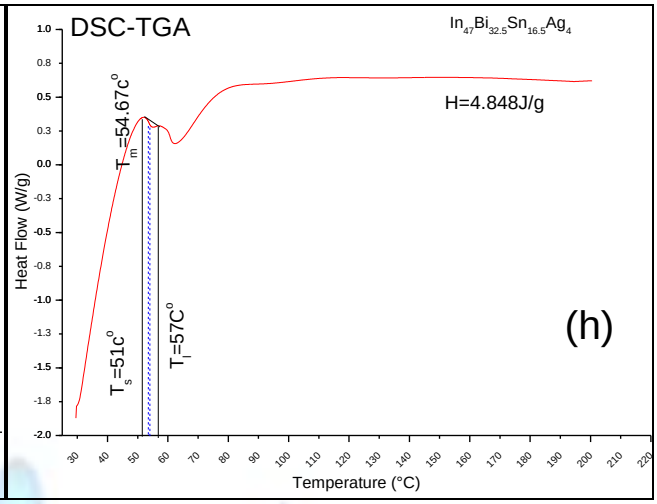

Fig. (3-h): DSC curve of In-32.5Bi-16.5Sn-4Ag

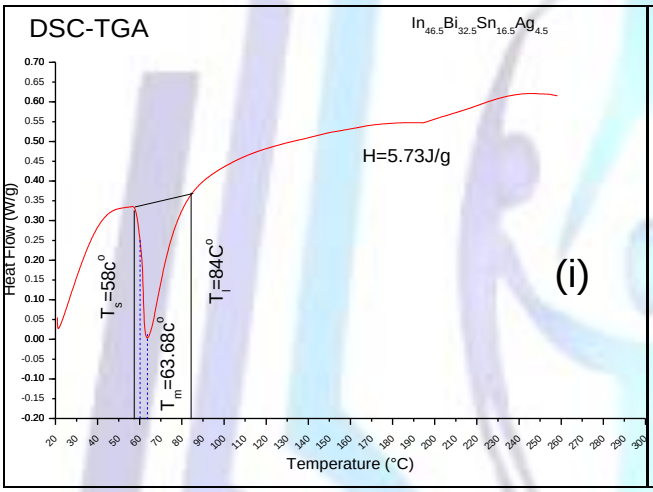

Fig. (3-i): DSC Curve of In-32.5Bi-16.5Sn-4.5Ag

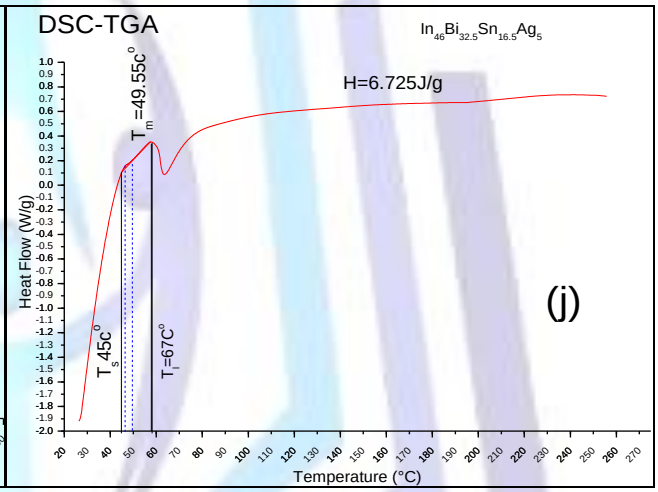

Fig. (3-j): DSC Curve of In-32.5Bi-16.5Sn-5Ag

Table (2): Thermal analysis of In-Bi-Sn-Ag melt spun alloys

System	T_s (K)	T_m (K)	T_l (K)	Pastry range (K)	Enthalpy (j/g)	Specific heat (j/g.K)	Entropy change (j/g.K)
$In_{50.5}$-$Bi_{32.5}$-$Sn_{16.5}$-$Ag_{0.5}$	330.5	332.90	341	10.5	9.80	0.9334	29.1990
In_{50}-$Bi_{32.5}$-$Sn_{16.5}$-Ag_1	329	332.10	348	19	8.68	0.4569	25.6569
$In_{49.5}$-$Bi3_{2.5}$-$Sn_{16.5}$-$Ag_{1.5}$	329.5	332.16	341	11.5	8.13	0.7073	24.2692
In_{49}-$Bi_{32.5}$-$Sn_{16.5}$-Ag_2	330	333.90	340	10	9.36	0.9357	27.9385
In_{48}-$Bi_{32.5}$-$Sn_{16.5}$-Ag_3	331	336.46	349	18	6.84	0.3802	20.1377
$In_{47.5}$-$Bi_{32.5}$-$Sn_{16.5}$-$Ag_{3.5}$	331	333.65	336	5	3.67	0.7346	11.0157
In_{47}-$Bi_{32.5}$-$Sn_{16.5}$-Ag_4	324	327.67	330	6	4.79	0.7990	14.6642
$In_{46.5}$-$Bi3_{2.5}$-$Sn_{16.5}$-$Ag_{4.5}$	331	336.68	357	26	5.73	0.2204	16.6679
In_{48}-$Bi_{32.5}$-$Sn_{16.5}$-Ag_5	318	322.55	330	12	6.73	0.5604	20.7623

ISSN 2347-3487

3.4. Mechanical properties

The dynamic resonance method has a definite advantage over static method of measuring elastic moduli because the low-level alternating stress does not inflate anelastic processes such as creep or elastic hysteresis [31]. The elastic moduli obtained with the resonance method give information about elastic compliances along the long axis of the melt-spun ribbons. In an elastically isotropic body such as a well prepared polycrystalline quenched ribbons, the elastic moduli are identical in any direction. Elastic moduli can be obtained from frequency f_o, at which peak damping occurs, according to:

$$E = \frac{38.32\rho l^4 f_o^2}{t^2} \quad \ldots\ldots\ldots\ldots\ldots\ldots (3)$$

$$G = \frac{E}{2(1+\nu)} \quad \ldots\ldots\ldots\ldots\ldots\ldots\ldots (4)$$

$$B = \frac{E}{3(1-2\nu)} \quad \ldots\ldots\ldots\ldots\ldots\ldots\ldots (5)$$

Where, E is elastic modulus (Young's modulus), ρ is ribbon density, l is vibrated part of ribbon, t is ribbon thickness, G is shear modulus, B is bulk modulus and v is Poisson's ratio. Fig (4) shows the Young's modulus of the melt quenched ribbons. It is evident that Young's modulus of eutectic In-Bi-Sn Field's metal [1] is increasing as the silver content increase. Young's modulus of eutectic In-Bi-Sn was 14.4 (Gpa) and with the addition of 3 wt. % of silver it was raised up to 16.6 (Gpa), or about 13% higher than the original value. The microhardness of eutectic Field's metal was also increase with increasing of silver content. Microhardness of the original In-Bi-Sn eutectic alloy was 175 Mpa [1]. The addition of Ag at 5 wt. % to Field's metal the microhardness increase to 198 (Mpa). This indicates the powerful effect of silver in improving Young's modulus and microhardness of Field's metal. The increasing of Young modulus and microhardness of this alloy can be explained by microstructure analysis of the alloy. From the microstructure analysis, it was found that In-rich phase is the basic microstructure of the original eutectic In-Bi-Sn-Ag alloy and intermetallic compounds between In, Sn, Ag and Bi such as BiSn, BiIn, In_3Sn, Ag_3Sn, $InSn_{19}$ are around the In rich phase. Another important characteristic of melt-spun ribbons can be calculated from frequency f_o, at which peak damping occurs which is internal friction (Q^{-1}). Internal friction measurements have been quite fruitful for learning the behavior of rapidly quenched ribbons from melt. It is one of the important characteristics which are indirectly related to their elastic properties. The free vibration is based on the measurement of the decay in amplitude of vibrations during free vibration. The internal friction is obtained by:

$$Q^{-1} = 0.5773\left(\frac{\Delta f}{f_o}\right) \quad \ldots\ldots\ldots\ldots (6)$$

Figures (5) and (6) show that both of microhardness and internal friction respectively with silver content.

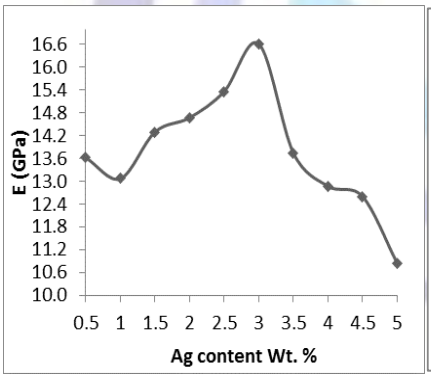

Fig (4): Young's modulus (E) Vs. Ag content

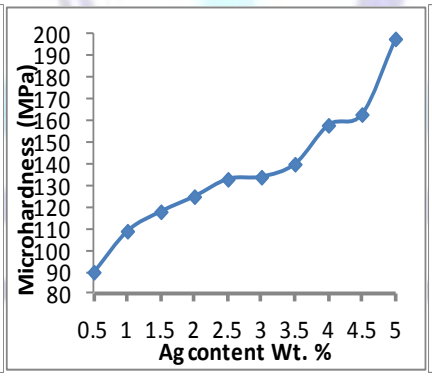

Fig (5): Microhardness Vs. Ag content

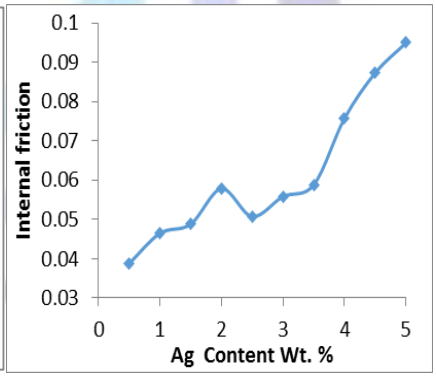

Fig (6): Internal friction Vs. Ag content

Ledbetter [32] and Gorecki [33] reported a theoretical basis for the experimental relationship between Young's modulus E and the shear modulus G which has recognized for many years:

$$G/E \approx 0.356 \quad \ldots\ldots\ldots\ldots (7)$$

So if we take into account the well-known relation between Young's modulus, the shear modulus and the bulk modulus:

$$G/E = \frac{(3 + G/B)}{9} \quad \ldots\ldots\ldots\ldots (8)$$

Table (3) below indicate the values of shear modulus, bulk modulus, Poisson's ratio and the parameters (G/E, G/B, E/B and ((3+(G/B))/9) for quenched ribbons, and that is obviously equations (7,8) are almost satisfied.

ISSN 2347-3487

Table 3: Shear modulus, bulk modulus, Poisson's ratio and G/E, G/B, E/B, (3+(G/B)/9) values

System	Shear modulus (Gpa)	Bulk modulus (GPa)	Poisson's ratio	G/E	G/B	E/B	(3+(G/B))/9
$In_{50.5}Bi_{32.5}Sn_{16.5}Ag_{0.5}$	5.1593	12.6116	0.3200	0.37879	0.40909	1.08000	0.37879
$In_{50}Bi_{32.5}Sn_{16.5}Ag_{1}$	4.9486	12.1195	0.3203	0.37870	0.40832	1.07820	0.37870
$In_{49.5}Bi_{32.5}Sn_{16.5}Ag_{1.5}$	5.4118	13.2876	0.3207	0.37859	0.40728	1.07580	0.37859
$In_{49}Bi_{32.5}Sn_{16.5}Ag_{2}$	5.5520	13.6578	0.3210	0.37850	0.40651	1.07400	0.37850
$In_{48.5}Bi_{32.5}Sn_{16.5}Ag_{2.5}$	5.8127	14.3353	0.3214	0.37839	0.40548	1.07160	0.37839
$In_{48}Bi_{32.5}Sn_{16.5}Ag_{3}$	6.2849	15.5295	0.3217	0.37830	0.40471	1.06980	0.37830
$In_{47.5}Bi_{32.5}Sn_{16.5}Ag_{3.5}$	5.1951	12.8695	0.3221	0.37819	0.40368	1.06740	0.37819
$In_{47}Bi_{32.5}Sn_{16.5}Ag_{4}$	4.8652	12.0753	0.3224	0.37810	0.40290	1.06560	0.37810
$In_{46.5}Bi_{32.5}Sn_{16.5}Ag_{4.5}$	4.7596	11.8434	0.3228	0.37799	0.40187	1.06320	0.37799
$In_{46}Bi_{32.5}Sn_{16.5}Ag_{5}$	4.0950	10.2093	0.3231	0.37790	0.40110	1.06140	0.37790

After computing elastic moduli, one can calculate the Debye temperature, which is an important fundamental parameter closely related to many physical properties such as elastic stiffness, specific heat and melting temperature .Low temperature specific heat is represented by a scalar parameter called the thermal Debye temperature θ_{Dt}, and the acoustic specific heat is represented by the acoustic Debye temperature θ_D .Thus at temperature near absolute zero:

$$\theta_{Dt} = \theta_D \quad \ldots\ldots\ldots\ldots\ldots\ldots\ldots\ldots (9)$$

The expression for the Debye temperature θ_D in terms of the sound velocities for an isotropic body is given by the following equation. [34-37]:

$$\theta_D = \frac{h}{k_B}\left(\frac{3}{4\pi V_a}\right) V_m \quad \ldots\ldots\ldots\ldots\ldots (10)$$

Where; h is the plank`s constant, k_B is the Boltzmann constant, V_a is the molar volume calculated from the effective molecular weight and density (i.e. $\frac{M}{\rho}$) and V_m is the mean ultrasonic velocity defined by the relation:

$$V_m = \frac{1}{3}\left(\frac{1}{V_l^3} + \frac{1}{V_t^3}\right)^{-\frac{1}{3}} \quad \ldots\ldots\ldots\ldots (11)$$

Where V_t and V_l are the transverse and longitudinal wave velocities in the solid defined by the relations:

$$V_t = \sqrt{\frac{G}{\rho}} \quad , V_l = \sqrt{\frac{3B - 4G}{3\rho}} \quad \ldots\ldots\ldots (12)$$

Where B is bulk modulus and G is the shear modulus. All previous parameters are tabulated in table (4).

Table 4: Transverse (V_t) and longitudinal (V_l) wave velocities, mean ultrasonic velocity (V_m) and Debye temperature (θ_D)

System	v_t (m s^{-1})	v_l (m s^{-1})	v_m(m s^{-1})	θ_D (K)
$In_{50.5}Bi_{32.5}Sn_{16.5}Ag_{0.5}$	1490.6308	2240.5422	455.9152	219.27
$In_{50}Bi_{32.5}Sn_{16.5}Ag_{1}$	1476.6942	2220.3535	451.6878	212.42
$In_{49.5}Bi_{32.5}Sn_{16.5}Ag_{1.5}$	1565.2529	2354.5869	478.8257	219.30
$In_{49}Bi_{32.5}Sn_{16.5}Ag_{2}$	1570.2514	2362.9191	480.3923	224.39
$In_{48.5}Bi_{32.5}Sn_{16.5}Ag_{2.5}$	1596.0721	2402.8797	488.3427	231.27
$In_{48}Bi_{32.5}Sn_{16.5}Ag_{3}$	1668.7699	2513.1960	510.6257	239.30
$In_{47.5}Bi_{32.5}Sn_{16.5}Ag_{3.5}$	1734.3147	2613.1175	530.7373	190.45
$In_{47}Bi_{32.5}Sn_{16.5}Ag_{4}$	1449.5356	2184.7977	443.6238	213.51
$In_{46.5}Bi_{32.5}Sn_{16.5}Ag_{4.5}$	1471.2151	2218.5076	450.3061	205.93
$In_{46}Bi_{32.5}Sn_{16.5}Ag_{5}$	1264.3993	1907.3098	387.0350	206.27

Conclusions

In this work, a new lead free solder "nontoxic" has been successfully stablished by chill-block melt-spin technique. The composition, morphology, microstructure, mechanical, and thermal properties were characterized. This study also provides a convenient and efficient route to prepare other soft solder formulation with low melting temperature (49.5 ^{o}C), for using in microelectronic applications. Addition of silver element can promote mechanical and thermal property of Field's metal in various ways. The melting temperature of Field's metal decreases after the addition of silver, this is due to the formation of near quaternary eutectic composition In-32.5 wt. % Bi-16.5 wt. % Sn-5 wt. % Ag. Due to the trends of multifunction, high speed, high power and/or miniaturization of microelectronic components such as LEDs having high luminance and central processing unit generate higher heat flow [13].This composition, In-32.5 wt. % Bi-16.5 wt. % Sn-5 wt. % Ag is characterized in that metal can be melted to the liquid state when heated, and the initial melting temperature therefore is below 50^{o}C, in comparison with the conventional Field's metal.

References

[1] M. Kamal, A. El-Bediwi, R. M. Shalaby, M. Younus. "A study of eutectic indium-bismuth and indium-bismuth-tin Field's metal rapidly solidified from melt". Journal of Advances in physics. Vol.7, No.2 (2015) PP. 1403-1413

[2] M. S. Bin jahari, "Properties of low temperature indium-based ternary lead free solder system" Thesis submitted in fulfilment of the requirements for the degree of Master of Science Universiti Sains Malaysia 2008

[3] Ruggiero, M.A., Rutter, J.W. "Origin of Microstructure in 350 K Eutectic of Bi-In-Sn Ternary System"; Mater. Sci. Technol., 11(2), 136-142 (1995).

[4] Stelmakh, S.I., Tsimmergakl, V.A., Sheka, I.A."The Compound In_2Bi"; Sov. Progr. Chem., 38, 631-633 (1972).

[5] Kabassis, H., Rutter, J.W., Winegard, W.C.'Microstructure of One of the Ternary Eutectic Alloys in the Bi-In-Sn System; Metall. Trans. A, 15A, 1515-1517 (1984).

[6] Kabassis, H., Rutter, J.W., Winegard, W.C. "Phase Relationships in Bi-In-Sn Alloy System". Mater. Sci. Technol., 2, 985-988 (1986).

[7] Ruggiero M. A.; Rutter J. W. "Origin of microstructure in the 332 K eutectic of the Bi-In-Sn system". Materials Science and Technology. Volume 13, Issue 1 (01 January 1997), pp. 5-11.

[8] Huang M. L., Zhou Q. Zhao N., Chen L. D. J Mater Sci: Mater Electron (2013) 24:2624–2629

[9]Yoon, S.W., Rho, B.-S., Lee, H.M., Kim, C.-U., Lee, B.-J. "Investigation of the Phase Equilibria in the Sn-Bi-In Alloy System". Metall. Mater. Trans. A, 30A, 1503-1515 (1999).

[10] Witusiewicz V.T., Hecht U., Bottger B., Rex S. Journal of Alloys and Compounds 428 PP.115–124.

[11] Adam Lipchitz, Glenn Harvel and Takeyoshi sunagawa 2013, Applied Mechanics and Materials, Vol420, issue 185-193.

[12] Mustafa kamal, Abu-bakr El-Bidiwi, Shalabia Badr and Sabah Taha, International Journal Of Engineering & Technology IJET-IJENS Vol. 12, No. 03 (2012) PP. 6-11

[13] Yuan-Giang Fann, Jen-Dong Hwang, Cheng-Chou Wong, United States Patent Application Publication. Pub. No.: US 2008/0110609 Al. Pub. Date: May 15, 2008

[14] Mustafa Kamal, Abu-Baker El-Bediwi and Tarek El-Ashram, Journal of Materials science in Electronics 15(2004) 211-217.

[15] Rizk Mustafa Shalaby and Mustafa Kamal, International Journal of physic and Research (IJPR), Vol.13, Issues, Dec. (2013), 51-60.

[16] Mustafa Kamal, Shalabia Badr and Nermin Ali Abdelhakim, International Journal of Engineering and Technology IJET-IJENS Vol: 14, No: 01 Feb. (2014) IJENS, PP: 119-129.

[17] Mustafa Kamal, Abu-Baker El-Bediwi and Jamal Khalil Majeed, International Journal of Engineering and Technology IJET-IJENS Vol.14, No: 02 April (2014) IJENS, PP: 5 -15.

[18] Mustafa Kamal and Usama S. Mohamed, A Review Chill-Block Melt spin Technique, Theoretical and Applications, EISBN: 978-1- 608005-151-9(2012), Bentham eBooks.

[19] H. H. Liebermann, Materials Science and Engineering, 43 (1980) 203-210.

[20] Y.A.Geller, A. G. Rakhshtadt,"Science of Materials, Mir publishers, Moscow, 1977, P. 138.

[21] A.M. Shaban and M. Kamal, Radiation Effects and Defects in Solids, (1995), Vol.133, PP: 5-13.

[22] Mustafa Kamal and Abu-Baker El-Bediwi, Radiation Effects and Defects in solids 174(1999)211.

[23] Pol Duwez, R. H. willens and W. Klement Jr., J. Appl. Phys.31, 1136 (1960).

[24] Pol Duwez, R. H. Willens, and W.Klement Jr., J. Appl. Phys.31, 1137(1960)

[25] Pol Duwez and R.H. Willens, Trans.Met .Soc. AIME 227, 326 (1963).

[26] B.D.Cullity, Elements of X-ray Diffraction, 2nd Edition (Addison- Wesely, 1978) p.248.

[27] D.Q Yu, J.Zhao, L.Wang, Journal of Alloys and Compounds 376(2004)170-175.

[28] R.M. Shalaby, Materials Science & Engineering A 560 (2013) 86–95

[29] B. Huang, N.C. Lee, Int. Symp. Microelectron. Proc. 3906 (1999) 711.

[30] F.Q. Zu, Z. G. Zhu, B. Zhang, Y. Feng and J.P. Shui, J. phys. Condens. Matter 13 (2001) 11435-11442.

[31] E. Schreiber, O. L. Anderson, and N. Soga, Elastic Constants and their Measurements, McGraw-Hill Book Company (1973) PP: 82-125.

[32] H. M. Ledbetter, Material Science and Engineering, 27(1977) 133.

[33] T. Gorecki, Material Science and Engineering, 43(1980) 225.

[34] Z. Sun, D. Music, R.Ahja, S. Li and J. M. Schneider, Phys.Rev. B70, 508(2004).

[35] O. L. Anderson, J. Phys.Chem .Solids 24,909 (1963).

[36] Morihiko Nakamura and Kazuhiro Kimura, Journal of Materials Science 26 (1991) 2208 2214.

[37] A.Bouhemadou, Brazilian Journal of Physics, Vol. 40, No.1 Sao Paulo Mar. (2010) PP: 1-10.